INVESTIGATION INTO HVDC CORONA: DISCUSSION AND INITIAL MODELLING RESULTS

A. G. Swanson[1*] and I. R. Jandrell[1]
[1]School of Electrical and Information Engineering, University of the Witwatersrand, 1 Jan Smuts Avenue, Johannesburg, South Africa
*E-mail: andrew.swanson@students.wits.ac.za

Abstract: Corona loss in transmission lines is caused by the partial breakdown of air around the conductor and the ion flow of charged particles away from the conductor. The manifestation of corona and the impact of corona loss varies according to electrode geometry, magnitude and distribution of the electric field and composition of the gas. As such it is important to account for corona in designing transmission lines as it has an impact on number of factors including: conductor size and rating, conductor bundles, and the selection of insulation. The object of the author's research is to investigate and model corona and in particular corona loss. The paper primarily identifies relevant available research, modelling techniques and published data with which the development of a corona model can be based and compared. In this case the 2 identified methods of modelling are the flux corrected transport algorithm and the particle mesh method. These 2 methods allows for a dynamic solution and are applicable to modelling of discharges or ion flow in a gaseous system. A basic solution of the particle mesh is implemented, however the solution is inaccurate and unstable for a number of reasons.

1 INTRODUCTION

The phenomena of corona in high voltage transmission line has been the interest of designers for a number of years, as it has an impact on the design of transmission lines, notably in the form of power (or corona) loss, audible noise, and electromagnetic and radio interference. There have been numerous studies on the impact of corona on transmission lines, including the development of empirical relationships based on measured data and more theoretical solutions based on the physical processes of the gas discharge phenomena. An often notable absence of corona theory for HVDC transmission lines is the inclusion of time-varying space charge, which, although highly complex, is important for power and energy loss, electromagnetic and radio interference.

The paper identifies some of the research and current theories for the physical processes of corona discharges and proposes a method to investigate the corona discharge process starting from the kinetic theory of gases through to the implementation of the ionization and corona theories for HVDC transmission lines. The ultimate goal of the research is to make use of the presently accepted theories and with the aid of measured data, particularly from coaxial corona cages, to develop an engineering solution for corona loss that can be applied to both unipolar and bipolar HVDC transmission lines.

2 HVDC CORONA

Under the influence of a electric field, electrons are accelerated in the direction of the field. These electrons may gain enough energy that on collision with another particle another electron may be released, these free electrons are subsequently accelerated and may release further electrons, resulting in an electron avalanche. In a uniform field when an electron avalanche becomes self sustaining and bridges a gap, breakdown occurs. In a non-uniform field, where the electric field intensity has a greater magnitude immediately surrounding the conductor and a lesser magnitude away from the conductor, a partial breakdown or corona may occur [1, 2].

For a non-uniform field, the avalanche becomes self-sustaining when [1, 2]:

$$n = n_0 \gamma e^{\int_0^d (\alpha - \eta) dx} \tag{1}$$

Where:
- α = Ionization coefficient
- η = Attachment coefficient
- γ = Secondary ionization coefficient

2.1 Negative Corona

For the cylindrical conductor with an applied high voltage under negative polarity as illustrated in figure 1. A nonuniform electric field distribution exists in the gap, with the highest value at the conductor surface. At a high enough voltage the electric field at the surface of the conductor becomes sufficiently high to initialise ionization. Naturally created free electrons initiate electron avalanches, which progress to a distance from the conductor where ionization and attachment are equal. Beyond the boundary all electrons attach to form negative ions. The impact of the positive ions on the conductor and photoionization produce the secondary ionization that causes a self-sustaining discharge or corona [2].

Following the initial electron avalanche, two ion space charge clouds (illustrated in figure 2) are formed from the positive and negative ions, moving towards the conductor and ground respectively. The space charge increase the electric field closer to the conductor and decreases the field away from the conductor, resulting in subsequent electron avalanches due to the higher field, but a shorter travelling distance for the avalanche [2].

Three modes of corona exist depending on the how the resultant space charge affects the electric field is modified, these include Trichel Streamer, Negative Glow and Negative Streamer. Each mode has distinct electrical, physical and visual manifestations [2].

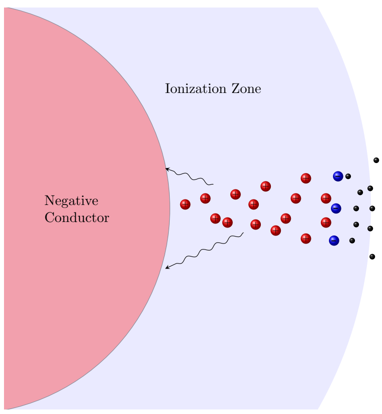

Figure 1: Negative Corona

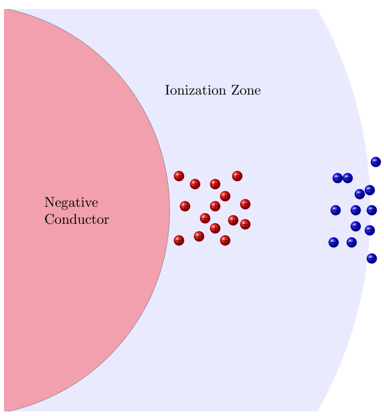

Figure 2: Negative Corona

2.2 Positive Corona

In the case of positive corona the electron avalanche is initiated by natural processes in the air at a boundary, where the ionization constant is greater than zero (illustrated in figure 3). The avalanche develops towards the conductor in the increasing electric field. The highest field-intensified ionization activity occurs near the conductor surface [2].

Secondary ionization occurs exclusively through photo-ionization. Clouds of space charge are formed by the various molecules in the gas, where most of the negative ions are created away from the conductor as electrons are neutralized closer to the conductor. These space charge clouds modify the electric field and the discharge development leading to various modes of corona including Burst Corona, Onset Streamer, Positive Corona and Breakdown Streamer [2].

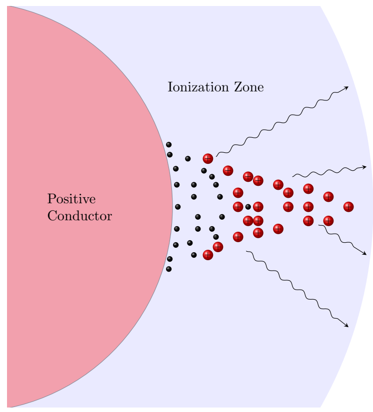

Figure 3: Positive Corona

2.3 AC and DC Corona

In investigating corona loss, coaxial corona cages are a useful tool in measuring the loss due to the alternating field of an AC conductor as the corona developed space charge tends to stay in the vicinity of the conductor. In direct current the space charge created by corona drifts away from the conductor filling the entire inter-electrode space. Coaxial corona cages are as such not useful in measuring corona loss on a DC system and applying this to other configurations such as overhead transmission lines.

3 CORONA MODELLING

Modelling techniques include both steady state solutions and time domain modelling, which generally revolve around the coupled solution of Poisson's equation and the continuity equation. The different techniques are discussed below.

3.1 Steady State Solutions

For corona loss involves the solution of Poisson's equation and the charge continuity equation, which are solved simultaneously by iterating through various values of space charge ρ until the solutions of the coupled equations converge. Common assumptions when modelling include [3–7]:

1. The mobility of ions is constant (independent of the field intensity and the drift time from generation),
2. Diffusion of ions is neglected,
3. The space charge affects only the magnitude but not the direction of the electric field. Known as Deutsch's assumption.
4. The ionization zone is neglected.
5. The electric field at the surface of the conductor remains constant at the onset voltage for corona. Known as Kapstov's Assumption.

The first assumption regarding the mobility of the ions is an averaged quantity that takes account of all the various ions that make up the gas. A constant or average mobility is used to simplify calculations. The mobility is independent of electric field, however this may not be the case in the ionization region as the successive avalanches are contributing to significantly to the thermal energy within the region which will in turn alter the kinetic energy of the gas [8].

Regarding the second assumption, Jones illustrates that the contribution of the diffusion to the velocity of ionic flow will be substantially smaller than the drift velocity and as such it is often neglected [8, 9].

The third assumption is used to transform two dimensional problems into one dimensional problems, by assuming that the space charge affects the magnitude of the electric field and not the direction (known as Deutch's assumption) [6]. It has been applied to cases for the solution of the steady state ion drift problem [5, 10]. In the case of the symmetrical coaxial arrangement, this assumption is not applicable as the Laplacian and Poission's field lines are the same.

The fourth assumption is used to simplify the solution as the ionization zone is generally significantly smaller than the ion drift zone, however in a time based solution this would provide a boundary condition for the production of ions from the corona discharge.

The fifth assumption is often used to simplify the solution for the ion drift problem and provide a boundary condition in solving the problem, however is known to be incorrect as the electric field will be altered by the production of space charge [11–14]. Additionally it cannot be constant in time as corona itself has a non constant nature, the space charge effect on the drift and plasma motion is shown in the solutions to the transport algorithm by Morrow and Lowke [15]. The alteration the electric field by a coronating conductor has been shown through measurements by Waters et al. [13]. Takuma et al. moved away from this assumption by using a constant charge density on the surface of the conductor [4].

3.2 Flux Corrected Transport Algorithm

Morrow et al. proposed the use of the flux corrected transport algorithm (initially described by Boris and Book) as a numerical solution to the flow of charged particles in a gaseous system [16–19]. Morrow and Lowke applied the algorithm for the modelling of a streamer [18]. The continuity equations can be rewritten for electrons, negative and positive ions in 1 dimension are given by:

$$\begin{aligned} \frac{\partial N_e}{\partial t} &= S + N_e\alpha|\vec{v}_e| - N_e\eta|\vec{v}_e| - N_eN_p\beta \\ &- \frac{\partial(N_e\vec{v}_e)}{\partial z} + \frac{\partial}{\partial z}\left(D\frac{\partial N_e}{\partial z}\right) \end{aligned} \tag{2}$$

$$\begin{aligned} \frac{\partial N_e}{\partial t} &= S + N_e\alpha|\vec{v}_e| - N_eN_p\beta - N_nN_p\beta \\ &- \frac{\partial(N_p\vec{v}_p)}{\partial z} \end{aligned} \tag{3}$$

$$\begin{aligned} \frac{\partial N_n}{\partial t} &= N_e\eta|\vec{v}_e| - N_nN_p\beta \\ &- \frac{\partial(N_n\vec{v}_n)}{\partial z} \end{aligned} \tag{4}$$

Where:

$N_{e/n/p}$	= Densities of electrons, negative ions and positive ions
$\vec{v}_{e/n/p}$	= Velocities of electrons, negative ions and positive ions [m.s^{-1}]
S	= Photoionization term
β	= Recombination coefficient
D	= Diffusion coefficient

Poisson's equation can be rewritten as:

$$\nabla^2\phi = -\frac{e^-}{\epsilon_0}(N_p + N_n + N_e) \tag{5}$$

Morrow et al. have used numerical methods including Finite Difference and Finite Elements Methods to solve the equations [18, 20].

3.3 Particle Mesh Method

The particle in cell technique represents numerous physical particles as a super particle. These super particles are moved and tracked in space from a Lagrangian point of view, weighted to a grid to solve for Poisson's equation, weighted to a particle and the cycle is repeated [21]. The technique has been applied to a number of gas discharge solutions [22–25].

3.3.1 Particle mover The particle mover uses the equations of motion to move the superparticle:

$$\frac{d\vec{x}}{dt} = \vec{v} \tag{6}$$

$$\frac{d\vec{v}}{dt} = \frac{q}{m}\vec{E} \tag{7}$$

In a discrete system these can be solve by explicit methods such as Euler 1st order method or the leapfrog 2nd order method, or a 4th order method such as Rugga-Kutta. The Euler method is the fastest method, but it is unstable under certain conditions, the leapfrog method is, however, more stable. The method is simple to implement and uses half time steps to calculate the position.

The solution of the equations of motion do not account for collisions with the background gas. Monte Carlo methods are the most suitable [21].

3.3.2 Particle and field weighting The simplest implementation of weighting is the zero order weighting of assigning all the charge to the nearest grid point (NGP). The scheme produces very noisy interpolation. A first order linear weighting scheme know as particle in cell or cloud in cell attempts to reduce the noisy interpolation by partially assigning the charge of the particles to grid points.

A third method, which is implemented in this paper, is to use a constant charge and have a variable area, this method is, however, prone to instabilities, errors and slower calculation times. In addition the technique is only implementable for a single charge species. The suitability will be discussed further on in the paper.

3.3.3 Accuracy, stability and noise There are a number of conditions that need to be satisfied in order for the solution to be accurate, stable and relatively noise free. As the super particles are representative of a greater number of physical particles, the greater the number of super particles the less noisy the solution.

Courant-Friedrichs-Lewy condition arises when solving an explicit algorithm [18]:

$$\Delta t < \frac{\Delta x}{W_e} \tag{8}$$

Debye length is a measure of the Debye shielding cloud that a charged particle carries around itself. Effectively it is a measure of how the charged particles will interact with each other [26]:

$$\lambda_D = \sqrt{\frac{\epsilon_0 k_B T}{n q_e^2}} \tag{9}$$

Where:
ϵ_0 = Permittivity of free space
k_B = Boltzmann's constant
n = Electron density
q_e = Electron charge

Particle oscillations, plasma frequency or Langmuir waves are the oscillations of the charged particles [26]:

$$w_p = \sqrt{\frac{n q_e^2}{\epsilon_0 m_e}} \tag{10}$$

Where:
m_e = Electron mass

The velocity of the electron can be related to the temperature [26]:

$$v_e = \sqrt{\frac{k_B T_e}{m_e}} \tag{11}$$

giving

$$w_p = \frac{v_e}{\lambda_D} \tag{12}$$

For accuracy and stability:

$$\Delta x < 3.4\lambda_D \tag{13}$$

$$\Delta t < 2 w_p^{-1} \tag{14}$$

4 MODEL VALIDATION

4.1 Model Setup

Morrow and Lowke implemented the drift and diffusion terms of equations 2 to 4 to study the effects of space-charge on electron and plasma motion in nitrogen. The plasma and system parameters include [18]:

- a pressure of 12 kPa,
- a temperature of 293 K,
- two electrodes 3cm apart, with the cathode at 0 cm and anode at 3 cm,
- a uniform electric field of -5.58 kV/cm,
- grid spacing, Δx, of less than 0.03 cm,
- time step, Δt, of 5×10^{-10} s

The electron density is described by a Gaussian distribution given by [18]:

$$N_e = N_0 e^{-\left(\frac{x-1.5}{0.25}\right)^2} \tag{15}$$

The electron velocity is given by [15]:

$$|W_e| = 9.56 \times 10^{21} E/N \tag{16}$$

Where:
N = Molecular concentration of the gas [cm^{-3}]
E = Electric field [V/cm]

There are a number of differences in the implementation, these include:

- Diffusion is ignored
- The solution of the electric field required boundary conditions on the electrodes, which alter the electric field across the gap and alter the movement of particles.

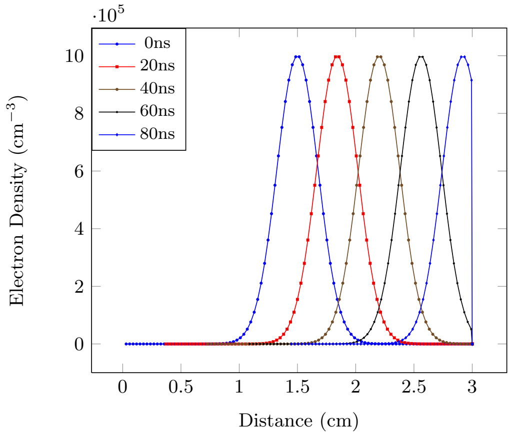

Figure 4: Space charge solution over time with $N_0 = 1 \times 10^6$ and $E_{applied} = 5.58$ kV/cm

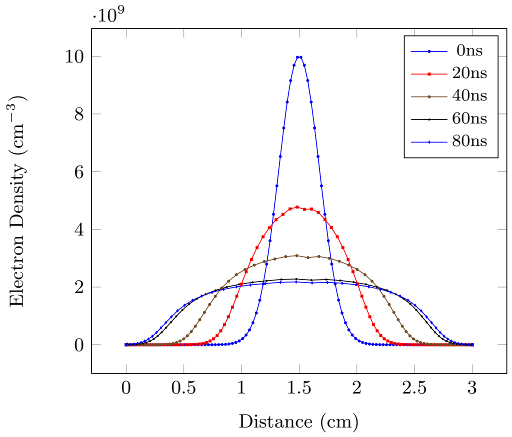

Figure 5: Space charge solution over time with $N_0 = 1 \times 10^{10}$ and $E_{applied} = 0$ kV/cm

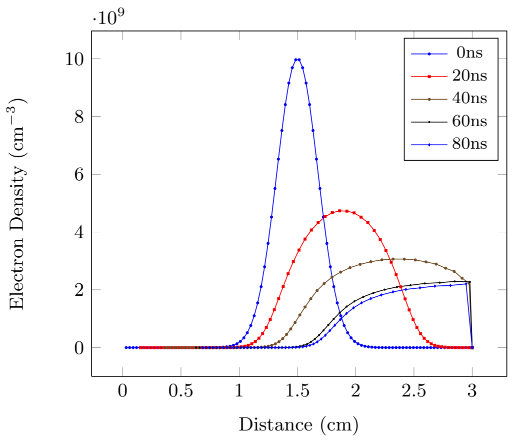

Figure 6: Space charge solution over time with $N_0 = 1 \times 10^{10}$ and $E_{applied} = 5.58$ kV/cm

Table 1: Parameters for method validation

Parameter	$N_e = 1 \times 10^6$	$N_e = 1 \times 10^{10}$
Grid spacing, Δx	0.0297	0.138

4.2 Results

5 DISCUSSION

Figure 4 illustrates the case with $N_0 = 1 \times 10^6$ where the applied electric field is significantly dominant over the electric field produced by the electron space charge. The results are similar to those produced by Morrow and Lowke. The implemented method is suitable as the original Gaussian distribution does not alter and as such the resolution and the grid space of the problem remain the same and do not exceed the stability and accuracy criteria.

Figure 5 illustrates the case with $N_0 = 1 \times 10^{10}$ where there is no applied electric field. In this case the electric field of the space charge has the effect of dispersing the electrons away from the center; the distribution remains Gaussian but has a smaller peak and fills a wider area. The higher the electric field the larger the velocity and subsequent movement, due the space charge affected the electric field in a non-uniform manner; larger grid sizes may result in certain areas leading to inaccuracies.

Figure 6 illustrates the case with $N_0 = 1 \times 10^{10}$ where the applied electric field is not dominant. In this case the electric field of the space charge has the effect of dispersing the electrons away from the centre and moving them in the direction of the field, the distribution not longer remains Gaussian and also has a smaller peak and fills a wider area.

The figures correspond in shape but not in magnitude to the results of Morrow and Lowke, this is due to the solution of Poisson's equation, where the electrodes required a bounded space to be solved.

The higher the electric field the larger the velocity and subsequent movement, due the space charge affected the electric field in a non-uniform manner; larger grid sizes will result (as shown in Table 1) leading to the solution exceeding the stability and accuracy limits shown previously.

6 CONCLUSION

The paper presented a discussion on modelling of corona, and presented some models that are useful.

The paper additionally presented a model, of which the implementation is not suitable for modelling of discharges and subsequently HVDC corona. The various error and stability criteria with which the model should comply are identified.

Future work includes:

- Correction of the model and validation against published results.
- Application to a non-uniform 1 dimensional field.

- Application to a non-uniform 2 dimensional field.
- Validation against 1 coaxial corona cage.

7 ACKNOWLEDGEMENTS

The authors would like to thank Eskom for the support of the High Voltage Engineering Research Group through the TESP programme. They would also like to thank CBI-electric for support, the department of Trade and Industry (DTI) for THRIP funding as well as to the National Research Foundation (NRF) for direct funding.

REFERENCES

[1] E. Kuffel, W. Zaengl, and J. Kuffel. *High Voltage Engineering: Fundamentals*. Newnes, second ed., 2000.

[2] P. Sarma Maruvada. *Corona Performance of High Voltage Transmission Lines*. Taylor and Francis Group, 2000.

[3] W. Janischewskyj and G. Gela. Finite element solution for electric fields of coronating DC transmission lines. *IEEE Transactions on Power Apparatus and Systems*, vol. PAS-98, no. 3, 1979.

[4] T. Takuma, T. Ikeda, and T. Kawamoto. Calculation of the ion flow fields of HVDC transmission lines by the finite element method. *IEEE Transactions on Power Apparatus and Systems*, vol. PAS-100, no. 12, 1981.

[5] P. Sarma Maruvada and W. Janischewskyj. Analysis of corona losses on DC transmission lines: I - Unipolar lines. *IEEE Transactions on Power Apparatus and Systems*, vol. 88, no. 5, 1969.

[6] J. Jones and M. Davies. A critique of the Deutsch assumption. *Journal of Physics D: Applied Physics*, vol. 25, 1992.

[7] J. Jones, J. Dupuy, G. Schreiber, and R. Waters. Boundary conditions for the positive direct-current corona in a coaxial system. *Journal of Physics D: Applied Physics*, vol. 21, 1988.

[8] J. Jones. On corona-induced gas motion and heating I: Field equations, modelling and vortex formation. *Journal of Electrostatics*, vol. 66, 2008.

[9] J. Jones. On the drift of gaseous ions. *Journal of Electrostatics*, vol. 27, 1992.

[10] P. Sarma Maruvada and W. Janischewskyj. Analysis of corona losses on DC transmission lines: II - Bipolar lines. *IEEE Transactions on Power Apparatus and Systems*, vol. 88, no. 10, 1969.

[11] P. Sarma Maruvada and W. Janischewskyj. DC corona on smooth conductors in air - Steady-state analysis of the ionisation layer. *Proceedings of the IEE*, vol. 116, no. 1, 1969.

[12] M. Khalifa and M. Abdel-Salam. Calculating the surface fields of conductors in corona. *Proceedings of the IEE*, vol. 120, no. 12, 1973.

[13] R. Waters, T. Rickard, and W. Stark. Direct measurement of electric field at line conductors during ac corona. *Proceedings of the IEE*, vol. 119, no. 6, 1972.

[14] M. Aboelsaad, L. Shafai, and M. Rashwan. Improved analytical method for computing unipolar DC corona losses. *IEE Proceedings A*, vol. 136, no. 1, 1989.

[15] R. Morrow and J. Lowke. Space-charge effects on drift dominated electron and plasma motion. *Journal of Physics D: Applied Physics*, 1981.

[16] R. Morrow. Numerical Solution of Hyperbolic Equations for Electron Drift in Strongly Non-uniform Electric Fields. *Journal of Computational Physics*, 1981.

[17] R. Morrow and L. Crem. Flux-Corrected Transport and Diffusion on a Non-uniform Mesh. *Journal of Computational Physics*, 1985.

[18] R. Morrow and J. Lowke. Streamer Propagation in Air. *Journal of Physics D: Applied Physics*, vol. 30, 1997.

[19] J. Boris and D. Book. Flux-corrected transport. I. SHASTA, a fluid transport algorithm that works. *Journal of Computational Physics*, 1973.

[20] G. Georghiou, R. Morrow, and A. Metaxas. An Improved Finite-Element Flux-Corrected Transport Algorithm. *Journal of Computational Physics*, vol. 148, 1999.

[21] C. Birdsall. Particle-in-Cell Charged Particle Simulations, Plus Monte Carlo Collisions with Neutral Atoms, PIC-MCC. *IEEE Transactions on Plasma Science*, vol. 19, no. 2, 1991.

[22] C. Soria, F. Pontiga, and A. Castellanos. Particle-in-Cell Simulation of Electrical Gas Discharges. *Journal of Computational Physics*, vol. 171, 2001.

[23] G. Lapenta, F. Iinoya, and J. Brackbill. Particle-in-Cell Simulation of Glow Discharges in Complex Geometries. *IEEE Transactions on Plasma Science*, vol. 23, no. 4, 1995.

[24] C. Li and C. Wu. Three Fluid Transport Models by Particle-in-Cell Method for RF Glow Discharges. *IEEE Transactions on Plasma Science*, vol. 20, no. 6, 1992.

[25] B. Qin, J. Sheng, Z. Yan, and G. Gela. Accurate Calculation of Ion Flow Field Under HVDC Bipolar Transmission Lines. *IEEE Transactions on Power Delivery*, vol. 3, no. 1, 1988.

[26] R. D. Blandford and K. S. Thorne. *Applications of Classical Physics*. California Institute of Technology, 2005.